SHIFTED CONTOUR AUXILIARY FIELD MONTE CARLO

ROI BAER

Chaim Weizmann Institute of Chemistry and Lise Meitner Center for Quantum Chemistry, the Hebrew University of Jerusalem, Jerusalem 91904 Israel.

DANIEL NEUHAUSER

Department of Chemistry and Biochemistry, University of California, Los Angeles CA 90095 USA.

Abstract

Shifted contour (SC) auxiliary field Monte Carlo (AFMC) for electronic structure is described in considerable algorithmic detail. Several applications demonstrate the high accuracy achievable in molecular electronic structure, including excited states, using the techniques of correlated sampling and variational AFMC. SC-AFMC is also applicable to large Hubbard lattices of strongly correlated electrons. Applications are shown, up to lattices of size 16×16 with 202 electrons. Finally, we present a method for exact coarse graining of the AFMC integrand.

1 Introduction

Drawing accurate chemical and physical properties of molecules directly out of theoretical equations is the great challenge of theoretical chemistry and condensed matter physics. One of the most problematic fields for such a feat is computational electronic structure. Here, several fundamental difficulties team up to make progress slow over the many years of activity. One major difficulty is the light mass of the electron, forcing us to use quantum mechanics. More so, the electronic wave function is a very complicated mathematical object. For many particles, such as for example the molecular nuclei, the ground state wave function is smooth and structureless. Not so for electrons! Because they are fermions, their wave functions are highly oscillatory since they must be antisymmetric with respect to electron exchange operations. To complicate life even more, for the results to have useful chemical significance, high precision is needed. For example, predicting reaction rates necessitates accurate activation energy barriers that are typically *small differences of very large energies*. Topping the difficulty tower, the usefulness of the methods relies not only on their accuracy but also on their applicability to large systems: methods are demanded for treating hundreds of electrons.

This chapter discusses a new theoretical method for electronic structure, which has a potential for achieving all the aforementioned goals. The method is the "shifted-contour auxiliary-field Monte Carlo". We show in this review several examples of SCAFMC capability for computing accurate energies *and energetic differences*. We demonstrate it is applicable to the electronic ground and excited states

of molecules. Finally, the favorable scaling capabilities of the method with system size are demonstrated even in cases of *strongly correlated* electrons by applying it to the 2 dimensional Hubbard model.

Monte Carlo methods for *quantum* many body systems, the Quantum Monte Carlo (QMC), were pioneered by Kalos[1,2] and McMillan[3]. It was quickly realized that for a general electronic system the QMC methods are very limited in their success. In fact, all known forms of fermion QMC methods suffer from a phenomenon generally known as "the fermion sign problem". Its origin is in the Pauli principle, which constrains the electronic wave function to be oscillatory in the electron $3N_e$ dimensional configuration space, where N_e is the number of electrons. The fermion sign problem makes the QMC computation for electrons exponentially difficult to converge: the computation time behaves as $T_{CPU} \sim e^{-\frac{1}{\varepsilon}}$, where ε is the accuracy. This is not the case with, for example, QMC computations of the groundstate of boson particles, where the convergence is polynomial, typically: $T_{CPU} \sim \frac{1}{\varepsilon^2}$. For different electron QMC methods the sign problem shows up in different ways. In the Kalos approach and the related diffusion Monte Carlo (DMC) methods[4], the sign problem shows up as our ignorance of the location of the nodes of the $3N_e$ dimensional wave function. If the exact location of the nodes was known, one could compute the groundstate energy exactly. This led Anderson to develop the fixed node approximation[5], which imposes the nodes of an approximate wave function (for example, the Hartree-Fock wave function).

The fixed node approximation allows quite accurate computations of the absolute electronic groundstate energy in molecules[4,6-9]. It has several severe drawbacks though. It is difficult, if not impossible, to correctly formulate a consistent derivative of the energy with respect to parameters in the Hamiltonian, for example, to compute the force on the nuclei[10] or other external field effects[11]. The sampling according to the nodes of the groundstate affects the efficiency of the computation of excited states [7]. Perhaps, the largest impact QMC has had on theoretical chemistry and condensed matter physics is due to the electron gas calculation of Ceperley and Alder[12], results of which are parameterized into all the various types of density functionals. Attempts to systematically improve upon the fixed node approximation[13] have proved very difficult because of the sign problem.

A different brand of QMC methods has emerges from the studies of strongly correlated electrons in periodic lattices, such as the Hubbard model[14]. The methods spawning from this problem are collectively called Auxiliary Field Monte Carlo methods (AFMC). AFMC is applicable to a wide range of many-body problems where the particles are pair-wise interacting – like electrons in a molecule.

The version of AFMC applicable to Hubbard lattice models was pioneered by Hirsch[15], and reviewed by Loh et al [16]. Recently a major development has enabled the application of this method to large lattice systems with very good precision[17,18].

A general Auxiliary-Field Monte Carlo method has also been developed by Sugiyama et al.[19]. Most applications of this version have been made within the study of nuclear structure and have been recently reviewed by Koonin *et al.*[20].

The application of AFMC to molecular electronic structure has met with great difficulties. A severe sign problem prevented any reasonable progress beyond 2-electron systems such as the Hydrogen molecule [21] or the He atom[22]. A major breakthrough was the recognition by Rom *et al.*[23] that there is an integration contour freedom in the Hubbard Stratonovich transformation, allowing a stabilization and moderation of the sign problem. Baer *et al.*[24] showed that there is an optimal choice of the contour shift, which cancels a dominant noisy term in AFMC. The resulting method, shifted-contour auxiliary-field Monte-Carlo (SC-AFMC) is the subject of this review.

We start by describing the SCAFMC in general terms. We then specialize to Hubbard models and in the final section of the review, we describe an implementation of the method using plane-waves and pseudopotentials, which allows highly accurate estimation of molecular structural and vibrational properties.

2 Basic Theory

The Hamiltonian of electrons in a molecule can be generally written in atomic units as :

$$H = -\frac{1}{2}\sum_n \nabla_n^2 - e^2 \sum_{n,A} \frac{Z_A}{r_{nA}} + \sum_n w(\mathbf{r}_n) + \frac{e^2}{2}\sum_{n\neq m}\frac{1}{r_{nm}}, \tag{2.1}$$

where lower and upper case indices are used to label coordinates of electrons and nuclei respectively and $w(\mathbf{r})$ is a potential of an external field operating on the system.

For further development, it is beneficial to use a 2nd-quantized form in which all quantities are described with reference to an orthonormal basis of real single particle orbitals $\phi_i(\mathbf{r})$. The basic operators are the electron creation and annihilation operators. The operator $\hat{c}_{js}^{\dagger}$ creates an electron of spin s (↑ or ↓) in orbital ϕ_j, while $\hat{c}_{js}$ annihilates an electron in this same state. Because electrons are fermions, these operators have the well-known anti-commutation relations[14] $\left[\hat{c}_{js}^{\dagger}, \hat{c}_{j's'}\right]_+ = \delta_{ss'}\delta_{jj'}$, $\left[\hat{c}_{js}, \hat{c}_{j's'}\right]_+ = \left[\hat{c}_{js}^{\dagger}, \hat{c}_{s'j'}^{\dagger}\right]_+ = 0$. Using the creation and destruction operators, the Hamiltonian can be written as:

$$\hat{H} = \sum_{ij,s} T_{ij}\hat{c}_{is}^{\dagger}\hat{c}_{js} + \frac{1}{2}\sum_{ijkl,s,s'} V_{ijkl}\hat{c}_{is}^{\dagger}\hat{c}_{ks'}^{\dagger}\hat{c}_{ls'}\hat{c}_{js}\ . \tag{2.2}$$

The parameters of the 2nd quantized Hamiltonian are then:

$$T_{ij} = \int \phi_i(\mathbf{r}) \hat{t} \phi_j(\mathbf{r}) d^3 r \,, \tag{2.3}$$

where:

$$\hat{t} = -\frac{1}{2}\nabla^2 - \sum_\alpha \frac{Z_\alpha e^2}{|\mathbf{r} - \mathbf{R}_\alpha|} + w(\mathbf{r}) \,, \tag{2.4}$$

and:

$$V_{ijkl} = \int \phi_i(\mathbf{r}) \phi_j(\mathbf{r}) v(\mathbf{r}, \mathbf{r}') \phi_k(\mathbf{r}') \phi_l(\mathbf{r}') d^3 r d^3 r' \,, \tag{2.5}$$

where:

$$v(\mathbf{r}, \mathbf{r}') = \frac{e^2}{|\mathbf{r} - \mathbf{r}'|} \,. \tag{2.6}$$

Our goal is to develop methods for computing various observables concerning the electrons. There are many options to strive for in this context. One of the most important observable, for studying the chemical properties of molecules, is the ground-state energy. Other important quantities are low-lying excited-state energies, charge distributions and AC/DC linear-response properties. Another worthy goal, useful particularly for large systems, is the electronic canonical partition function $Z_c(\beta, N_e) = tr_{N_e}\left\{e^{-\beta \hat{H}}\right\}$ from which the thermodynamic properties of the electrons may be inferred.

In most of these objectives, the Boltzmann operator $e^{-\beta \hat{H}}$ plays a central role. With a large inverse temperature, it can be used to project the low energy manifold of the molecule. For higher temperatures, it can be used to compute the partition function or to trace thermodynamic expectation values. We therefore concentrate in this review on the development of computational methods for accurately estimating matrix elements of the Boltzmann operator. Our goal is towards the low temperatures (large β values).

It is convenient to use the friendliest, N_e-electron wavefunctions - the Slater determinants. These wavefunctions describe N_e electrons that are occupying a set of N_e spin-orbitals $f_1(\mathbf{x}) \ldots f_{N_e}(\mathbf{x})$ where $\mathbf{x} \equiv (\mathbf{r}, \xi)$ is a space-spin single electron coordinate:

$$\Phi_f(\mathbf{x}_1, \ldots, \mathbf{x}_{N_e}) = \frac{1}{\sqrt{N_e!}} \begin{vmatrix} f_1(\mathbf{x}_1) & \cdots & f_1(\mathbf{x}_{N_e}) \\ \vdots & \ddots & \vdots \\ f_1(\mathbf{x}_1) & \cdots & f_{N_e}(\mathbf{x}_{N_e}) \end{vmatrix} . \tag{2.7}$$

In terms of our orthonormal basis orbitals, $\phi_i(\mathbf{r})$, we may write:

$$f_\alpha(\mathbf{x}) = \sum_{\substack{j=1 \\ s=\uparrow\downarrow}}^{N} \phi_j(\mathbf{r}) \delta_{s\xi} F_{js,\alpha} \quad \alpha = 1 \ldots N_e \,. \tag{2.8}$$

The expansion constants $F_{js,\alpha}$ form a rectangular matrix of numbers. In the 2nd quantization picture, we define the creation operators:

$$f_\alpha^\dagger = \sum_j c_{js}^\dagger F_{js,\alpha}\,, \tag{2.9}$$

with which we define the 2nd quantization analog of the determinantal wave function:

$$\Phi_{f_1\cdots f_{N_e}} \Leftrightarrow f_1^\dagger \cdots f_{N_e}^\dagger \left|0\right\rangle. \tag{2.10}$$

As described above, our general goal is then to develop a computational scheme enabling the computation of the Boltzmann operator matrix elements:

$$\left\langle \Phi_g \left| e^{-\beta\hat{H}} \right| \Phi_f \right\rangle = \left\langle 0 \left| g_{N_e} \cdots g_1 e^{-\beta\hat{H}} f_1^\dagger \cdots f_{N_e}^\dagger \right| 0 \right\rangle. \tag{2.11}$$

These quantities will be used in this chapter to mainly compute the groundstate energy of the molecule:

$$E_{gs} = \lim_{\beta\to\infty} \frac{\left\langle \Phi_g \left| \hat{H} e^{-\beta\hat{H}} \right| \Phi_f \right\rangle}{\left\langle \Phi_g \left| e^{-\beta\hat{H}} \right| \Phi_f \right\rangle}, \tag{2.12}$$

where Φ_f and Φ_g are any determinantal wave functions not orthogonal to the true ground state.

2.1 The essence of the problem

In order to appreciate the character of our problem, we first consider a tractable case. Suppose that the Hamiltonian contains only one-body interactions. That is, take $\hat{H} = \hat{T}$ in Eq. (2.2). In this case, when the Boltzmann function operates on a determinantal wave function $\Phi_{f_1\cdots f_{Ne}}$, the result is once again a determinantal wave function. Explicitly, it is given by $\Phi(\beta) = e^{-\beta\hat{T}}\Phi_f = \Phi_{f(\beta)}$ - i.e. the determinantal wave function is composed of the orbitals $f_n(\beta) = e^{-\beta\hat{t}} f_n$. It is quite straightforward to understand why this is so. Assume the orbitals are orthonormal (this is not essential, just convenient). The wavefunction $\Phi(\beta) = e^{-\beta\hat{T}}\Phi_f$ solves the differential equation:

$$\frac{d\Phi(\beta)}{d\beta} = -\hat{T}\Phi(\beta) \qquad \Phi(\beta) = \Phi_f\ . \tag{2.13}$$

We show that $\Phi(\beta) = \Phi_{f(\beta)}$ leads to an acceptable solution, which because of uniqueness is the only solution. For this, substitute $\Phi(\beta) = \Phi_{f(\beta)}$ on both sides of

(2.13) and multiply by $\prod_{\substack{k=1 \\ k\neq m}}^{N_e} f_k(\beta,\mathbf{r}_k)$ integrating over all $\mathbf{r}_k$, for which $k \neq m$. This procedure leaves the following differential equation, which $f_m(\beta)$ must solve:

$$\frac{df_m}{d\beta} = -\hat{t}f_m , \tag{2.14}$$

proving that indeed $f_n(\beta) = e^{-\beta\hat{t}} f_n$. This mathematical fact just reflects the physical situation that when the particles do not interact with each other, they respond to one-body Hamiltonians in a completely independent way.

The reader should appreciate that this is quite a remarkable result, by no means trivial. It has far-reaching consequences. The Boltzmann operator of a one-body Hamiltonian $\hat{T}$ is a *many-body* operator, i.e. it has 2-body, 3-body etc., terms built into it – as can be seen by simply expanding it in a Taylor type series $e^{-\beta\hat{T}} = \sum_{n=0}^{\infty}\left(-\beta\hat{T}\right)^n \Big/ n!$. Yet, its operation on a determinant is remarkably simple: the wavefunction stays a determinant!

All this simplicity is erased however, when a two-body interaction is present. Now the particles are dependent. The picture is complicated. Starting from a determinant at $\beta = 0$, the wavefunction at any $\beta > 0$ is not simple at all it is a linear combination of a large number of determinants. The number of possible determinants grows very rapidly, factorially, with system size and with number of electrons and exponentially with β.

2.2 The Hubbard-Stratonovich Transformation

It should now be apparent, that any mathematical manipulation that allows the complete elimination of electron-electron interaction without making any approximation, leaving only one-body Hamiltonians - is of tremendous importance. This is just what the Hubbard–Stratonovich transformation accomplishes. We now describe the basic theory, using 2nd quantization formalism.

Since the matrices *T* and *V* of Eqs. (2.3) or (2.5) defining the interaction do not reference spin, it is useful to eliminate explicit reference from the formalism. Let us then introduce the density matrix operator, with elements:

$$\hat{\rho}_{ij} = \sum_{s=\uparrow\downarrow} \hat{c}_{si}^{\dagger}\hat{c}_{sj} \quad \hat{\rho}_{ij}^{\dagger} = \hat{\rho}_{ji} . \tag{2.15}$$

The Hamiltonian of Eq. (2.2) can then be written directly in terms of the density matrix:

$$\hat{H} = \sum_{ij} t_{ij}\hat{\rho}_{ij} + \frac{1}{2}\sum_{ijkl} \hat{\rho}_{ij} V_{ijkl} \hat{\rho}_{kl} , \tag{2.16}$$

with:

$$t_{ij} = T_{ij} - \frac{1}{2}\sum_l V_{illj} \ . \tag{2.17}$$

Next, let us use a shorthand notation, defining the composite index $I = (ij)$ (sometimes we will also write $K = (kl)$) and write the Hamiltonian in the following elegant way:

$$\hat{H} = t^T \hat{\rho} + \frac{1}{2}\hat{\rho}^T V \rho \, . \tag{2.18}$$

Here, t and $\hat{\rho}$ are considered column vectors of some dimension $M = N \times N$ in the index *I*, respectively of the elements:

$$t_I = t_{ij} \qquad \hat{\rho}_I = \hat{\rho}_{ij} \, . \tag{2.19}$$

The elements of matrix V are defined as follows:

$$V_{IK} = V_{ijkl} \, . \tag{2.20}$$

We use the mathematical notation:

$$A^T B = \sum_I A_I B_I \ . \tag{2.21}$$

A particularly important fact concerning the matrix V_{IK} is that it is "positive definite", a fancy name for saying that all its eigenvalues are positive. Physically this comes from the simple fact that electrons repel each other with an ever-positive monotonically decreasing e^2/r_{12} potential. Mathematically, this can be proved by showing that V_{IK} is an *overlap matrix* $V_{IK} = \langle G_I | G_K \rangle$ for some set of functions G_I. Overlap matrices are always positive definite: they can be diagonalized by simply orthogonalizing the functions G_I. Their eigenvalues are then just the norms of the orthogonal functions and norms are always positive!

By going to Fourier space, we can find exactly what the functions G_I that form the matrix V_{IK} are. Define:

$$\begin{aligned} F_K(\mathbf{q}) &= (2\pi)^{-3} \int e^{i\mathbf{q}\cdot\mathbf{r}} \phi_k(\mathbf{r}) \phi_l(\mathbf{r}) d^3 r \\ \phi_k(\mathbf{r}) \phi_l(\mathbf{r}) &= \int F_K(\mathbf{q}) e^{-i\mathbf{q}\cdot\mathbf{r}} d^3\mathbf{q} \end{aligned} \ . \tag{2.22}$$

Next, use the fact that for $q \neq 0$:

$$\int \frac{e^{i\mathbf{q}\cdot\mathbf{r}}}{r} d^3 r = \frac{4\pi}{q^2} \, . \tag{2.23}$$

And then:

$$V_{IK} = 4\pi e^2 \langle q^{-1} F_I | q^{-1} F_K \rangle \, , \tag{2.24}$$

showing that V_{IK} is an overlap matrix composed of the functions $G_I(\mathbf{q}) = \sqrt{4\pi e^2}\, q^{-1} F_I(q)$ and therefore it must be positive definite.

The positive definiteness property of V_{IK} means that for any vector σ_I of real components, the following inequality holds:

$$\sigma^T V \sigma = \sum_{IK} \sigma_I V_{IK} \sigma_K \geq 0 \,. \tag{2.25}$$

We now consider the Boltzmann propagator. We decompose, using the Suzuki-Trotter formula:

$$e^{-\beta H} = e^{-\Delta\beta H} e^{-\Delta\beta H} \cdots e^{-\Delta\beta H} \,. \tag{2.26}$$

Here, $\Delta\beta = \beta / L$ where L is the number of time-slices, an integer. We can now formally use the above decomposition keeping only first order contributions in $\Delta\beta$, taking the limit $L \to \infty$ at the end of the manipulations. Treating a single time slice, we may separate the one-body and two-body parts as follows:

$$e^{-\Delta\beta \hat{H}} \left| \Phi_f \right\rangle \approx e^{-\Delta\beta t^T \hat{\rho}} e^{-\Delta\beta \frac{1}{2} \hat{\rho}^T V \hat{\rho}} \left| \Phi_f \right\rangle \,. \tag{2.27}$$

Because the one-body and two body parts are not commutative, this introduces an error proportional to $\Delta\beta^2$. The effects of this error will not be noticed in the limit $\Delta\beta \to 0$. We now consider the problematic term:

$$e^{-\Delta\beta \hat{V}} \left| \Phi_f \right\rangle = e^{-\Delta\beta \left(\hat{\rho}^T V \hat{\rho} \right)} \left| \Phi_f \right\rangle \,. \tag{2.28}$$

To effectively remove the two body interactions, replacing them with 1-body interactions, we use the Hubbard-Stratonovich transformation. It is based on the fact that the Fourier transform of a Gaussian is a Gaussian, thus if $v > 0$:

$$e^{-\frac{1}{2} v x^2} = \sqrt{v / 2\pi} \int_{-\infty}^{\infty} e^{-\frac{1}{2} v \sigma^2} e^{-iv\sigma x} d\sigma \,. \tag{2.29}$$

Generalized to the case of an *M*-dimensional integral with *V* a *M*×*M* positive definite matrix, we have:

$$e^{-\frac{1}{2} x^T V x} = \sqrt{(2\pi)^{-M} \det V} \int e^{-\frac{1}{2} \sigma^T V \sigma} e^{-i \sigma^T V x} d^M \sigma \,. \tag{2.30}$$

Next, we plug, instead of the *numerical* vector x_I, the vector of density matrix elements $\hat{\rho}_I$:

$$\exp\left(-\tfrac{1}{2} \hat{\rho}^T V \hat{\rho} \Delta\beta \right) \approx C \int \exp\left(-\tfrac{1}{2} \sigma^T V \sigma \Delta\beta \right) \exp\left(-i \sigma^T V \hat{\rho} \Delta\beta \right) d^M \sigma \tag{2.31}$$

with:

$$C = \sqrt{\det\left[V \Delta\beta / 2\pi \right]} \,. \tag{2.32}$$

Note that Eq. (2.31) holds to only first order in $\Delta\beta$ because of the different components of $\hat{\rho}$ do not commute. This is the meaning of the $\approx$ sign. This equation is the central result of the Hubbard-Stratonovich theory, it shows how the Boltzmann operator of a 2-body Hamiltonian $\hat{\rho}^T V \hat{\rho}$ is converted into a weighted sum of evolu-

tion operators of a 1-body Hamiltonian $\sigma^T V\hat{\rho}$. The integral is over all possible *M*-dimensional "density vectors" σ_I. Putting all the *L* time-slices together, we have:

$$\begin{aligned}\left\langle \Phi_g \left| e^{-\beta H} \right| \Phi_f \right\rangle &= \left\langle \Phi_g \left| e^{-\Delta\beta H} e^{-\Delta\beta H} \cdots e^{-\Delta\beta H} \right| \Phi_f \right\rangle \\ &\approx C^L \int d^M\sigma_1 \cdots d^M\sigma_L \exp\left(-\tfrac{1}{2}\sum_{l=1}^{L} \sigma_l^T V \sigma_l \Delta\beta \right) \times \left\langle \Phi_g \left| \hat{U}_{\sigma_L} \cdots \hat{U}_{\sigma_1} \right| \Phi_f \right\rangle\end{aligned}, \tag{2.33}$$

where the single-body Hamiltonian evolution operator is,

$$\hat{U}_\sigma = \exp\left(-\Delta\beta \left(t + iV\sigma \right)^T \hat{\rho} \right). \tag{2.34}$$

In the limit of $L \to \infty$ (where *L* is the number of time slices) Eq. (2.33) is exact. When Φ and Ψ are determinantal wavefunctions, these expressions become computationally tractable forming the Hubbard-Stratonovich expression of the matrix elements of the Boltzmann operator.

2.3 Computational scheme based on Monte Carlo

The multidimensional functional integrals in Eq. (2.33) can be performed by Monte-Carlo integration. For this to be apparent, we rewrite (2.33) in the following way:

$$\begin{aligned}&\left\langle \Phi_g \left| e^{-\beta H} \right| \Phi_f \right\rangle \approx \\ &\qquad \int W\left[\sigma\right] \left\langle \Phi_g \left| \hat{U}_{\sigma_L} \cdots \hat{U}_{\sigma_1} \right| \Phi_f \right\rangle D\sigma\end{aligned}. \tag{2.35}$$

where:

$$W\left[\sigma\right] = \frac{e^{-\frac{1}{2}\sum_{l=1}^{L} \sigma_l^T V \sigma_l \Delta\beta}}{\int e^{-\frac{1}{2}\sum_{l=1}^{L} \sigma_l^T V \sigma_l \Delta\beta} D\sigma}. \tag{2.36}$$

In a similar way, an energy element can be written as:

$$\begin{aligned}&\left\langle \Phi_g \left| \hat{H} e^{-\beta\hat{H}} \right| \Phi_f \right\rangle \approx \\ &\qquad \int W\left[\sigma\right] \left\langle \Phi_g \left| \hat{H}\hat{U}_{\sigma_L} \cdots \hat{U}_{\sigma_1} \right| \Phi_f \right\rangle D\sigma\end{aligned}. \tag{2.37}$$

Let us now sketch the algorithm for computing the overlap and energy of a molecule. In a single reference case the two determinants on the left and right are identical and we define:

$$S\left(\beta\right) = \left\langle \Phi_f \left| e^{-\beta\hat{H}} \right| \Phi_f \right\rangle, \tag{2.38}$$

$$H\left(\beta\right) = \left\langle \Phi_f \left| \hat{H} e^{-\beta\hat{H}} \right| \Phi_f \right\rangle. \tag{2.39}$$

Note that in principle, $H\left(\beta\right) = -dS/d\beta$, however we will describe a direct method too. Once these quantities are known, the ground state energy can be approximated as:

$$E_{gs} = \lim_{\beta\to\infty} E(\beta) = \lim_{\beta\to\infty} \frac{H(\beta)}{S(\beta)}. \tag{2.40}$$

Algorithm (AFMC)

1) Basis application on the Hartree-Fock molecular orbitals: $f_\alpha(\mathbf{r}) = \sum_i \phi_i(\mathbf{r}) F_{i\alpha}$. Set iteration counter $N_{iter} = 0$.

2) Set time step l = 0. Set the $N\times N$ matrix $\mathbf{U} = \mathbf{I}$.

3) Generate a random vector-density σ_I (I = 1 … M) that is distributed according to a Gaussian distribution $\exp\left(-\frac{1}{2}\sigma^T V \sigma \Delta\beta\right)$. This is done by first determining M random numbers γ_I sampled from a Gaussian distribution of zero mean and unit variance ($\mu = 0$, $\sigma^2 = 1$). Then, $\sigma_I = \sum_{J=1}^{M} \left(\mathbf{L}^{-1}\right)_{IJ} \gamma_J$ where $\mathbf{L}$ is a lower triangular matrix (and therefore easily invertible) obtained from the Cholesky[25] factorization $V = \mathbf{L}^T\mathbf{L}$.

4) Create the Hamiltonian:

$$\left(\mathbf{h}_\sigma\right)_{ij} = \left(\mathbf{h}_\sigma\right)_I = t_I + i\sum_K V_{I,K}\sigma_K \ . \tag{2.41}$$

5) Update $\mathbf{U} \leftarrow \mathbf{U}_\sigma\mathbf{U}$, where $\mathbf{U}_\sigma = e^{-\mathbf{h}_\sigma\Delta\beta}$ is the evolution matrix corresponding to the evolution operator of Eq. (2.34). The exponential of a matrix may be computed either using a polynomial expansion or directly by diagonalizing. Thus, if $\mathbf{h}_\sigma = D^{-1}\mathbf{e}D$ where $\mathbf{e}$ is a diagonal matrix of eigenvalues. Then $\mathbf{U}_\sigma = D^{-1}e^{-\Delta\beta\mathbf{e}}D$, where $e^{-\Delta\beta\mathbf{e}}$ is the diagonal matrix with elements $\mathbf{u}_i = e^{-\Delta\beta\mathbf{e}_i}$

6) $l \leftarrow l + 1$. If $l < L$ go to step 3.

7) Compute $S \leftarrow S + \det\mathbf{F}^\dagger\mathbf{U}\mathbf{F}$ (the reader is referred to the appendix for details on matrix element evaluation). Notice that the factors $\prod_{l=0}^{L-1}\left(Cd^M\sigma_l\right)$ in Eq. (2.33) are already contained implicitly since the random numbers are drawn from normalized distributions.

8) Update average $S \leftarrow \frac{S\times N_{iter} + \det\mathbf{F}^\dagger\mathbf{U}\mathbf{F}}{N_{iter}+1}$ and iteration number

$$N_{iter} \leftarrow N_{iter} + 1 .$$

2.4 The dominant sign problem in AFMC

Applying this straightforward algorithm to the simplest system: a 2 site Hubbard model reveals a severe problem, as seen in FIG. 1. The signal to noise ratio of the AFMC computation exponentially explodes. This is a manifestation of the sign problem. It may come as a surprise since the 2-site 2-electron system is considered to not have a sign problem. The exact wave function is nodeless. Real-space discrete AFMC is known not to suffer from the sign problem for the half filled Hubbard model. Still, it is seen that for the complex continuous AFMC method there is a severe sign problem, known more accurately as the phase problem.

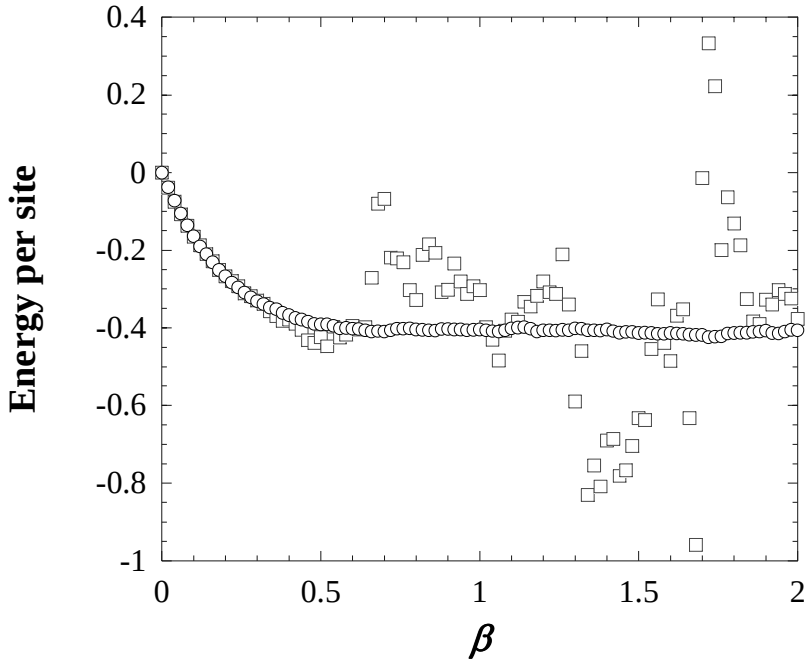

FIG. 1 AFMC (squares) and SCAFMC (circles) energies of the 2-site 2-electron Hubbard model as a function of the inverse temperature, after 16000 iterations. $\delta t = 0.02$. $U = 4$, $t = 1$.

The computation of the energy expectation value is concerned with computing the quotient of two Monte Carlo estimated quantities (Eq. (2.40)). Yet, because formally the numerator is the derivative of the denominator:

$$H(\beta) = -\frac{dS(\beta)}{d\beta}. \tag{2.42}$$

In order to understand the origins of the sign problem in AFMC, it suffices to consider only $S(\beta)$. Let us analyze the statistical properties of a single time-step:

$$\begin{aligned} S(\beta) &= \left\langle \left\langle \Phi_g \left| e^{-\Delta\beta(t+iV\sigma)^T \hat{\rho}} \right| \Phi_f \right\rangle \right\rangle_{W(\sigma)} \\ &= \left\langle \left\langle \Phi_g \left| 1 - i\Delta\beta\sigma^T V \hat{\rho} \right| \Phi_f \right\rangle \right\rangle_{W(\sigma)} + O(\Delta\beta). \\ &= \left\langle \Phi_g \left| 1 - i\Delta\beta \left\langle \sigma^T \right\rangle_W V \hat{\rho} \right| \Phi_f \right\rangle + O(\Delta\beta) \end{aligned} \tag{2.43}$$

The middle term is zero because $\langle\sigma\rangle = 0$. However, it has fluctuations. The Gaussian distribution ensures that $\left\langle \sigma^T V \sigma \right\rangle \Delta\beta \approx 1$, so the fluctuations are of magnitude proportional to $\sqrt{\Delta\beta}$. Apart from the constant term $\langle\Psi|\Phi\rangle$, the dominant part of the signal is proportional to $\Delta\beta$. Thus, the noise to signal ratio is:

$$\frac{\text{noise}}{\text{signal}} \propto \frac{1}{\sqrt{\Delta\beta}}, \tag{2.44}$$

which is formally infinite.

2.5 The cure: contour shift

Interestingly, there is a simple cure to this problem analytically nullifying the spurious term of the previous section. Rom et al.[23], point out that the Hubbard-Stratonovich transformation carries a certain freedom in its definition. For example, going back to Eq. (2.29), one may shift the integration contour by α:

$$\exp\left(-\tfrac{1}{2}vx^2\right) = \sqrt{v/2\pi} \int_{-\infty-i\alpha}^{\infty-i\alpha} \exp\left(-\tfrac{1}{2}v\sigma^2\right)\exp\left(-iv\sigma x\right) d\sigma. \tag{2.45}$$

One can check the validity Eq. (2.45) by straightforward integration. Now, in the *M*-dimensional case, one may shift each σ_I by any amount α_I. Inserting into Eq. (2.31), we obtain:

$$\begin{aligned} \exp\left(-\tfrac{1}{2}\hat{\rho}^T V \hat{\rho}\Delta\beta\right) \approx Ce^{\frac{1}{2}\alpha^T V\alpha\Delta\beta} \int \exp\left(-\tfrac{1}{2}\sigma^T V\sigma\Delta\beta\right) \times \\ \exp\left(i\sigma^T V\alpha\Delta\beta\right)\exp\left(-i\left(\sigma - i\alpha\right)^T V\hat{\rho}\Delta\beta\right) d^M\sigma \end{aligned}. \tag{2.46}$$

Performing the same analysis as in Eq. (2.43), one sees that by choosing the shift at time t to equal the density matrix element at that time:

$$\alpha_I = \left\langle \Phi_g(t) \left| \hat{\rho}_I \right| \Phi_f(t) \right\rangle, \tag{2.47}$$

the noisy term is analytically cancelled from the integrand. Even if the density matrix elements are not know exactly, much of the effect of the noisy term can be

mitigated by simply choosing a good approximation. The shifted contour procedure gives rise to the following algorithm:

Algorithm (SC-AFMC)

1) Basis application to the Hartree-Fock molecular orbitals: $f_\alpha(\mathbf{r}) = \sum_i \phi_i(\mathbf{r}) F_{i\alpha} \quad \alpha = 1, \cdots, N_e$. Set iteration counter $N_{\text{iter}} = 0$. Note, that in a closed shell computation there will be $N_e/2$ orbitals.

2) Determine contour shift as the Hartree-Fock density matrix: $\alpha_I = \alpha_{ij} = \sum_{\alpha=1}^{N_e} F_{i\alpha} F_{j\alpha}$.

3) Set time step $l = 0$. Set the $N \times N$ matrix $\mathbf{U} = \mathbf{I}$.

4) Generate a random vector-density σ_I (I = 1 … M) that is distributed according to a Gaussian distribution $\exp\left(-\frac{1}{2}\sigma^T V \sigma \Delta\beta\right)$ (see step 3 in the AFMC algorithm of the previous section).

5) Create the Hamiltonian

$$\begin{aligned}(\mathbf{h}_\sigma)_{ij} &= (\mathbf{h}_\sigma)_I \\ &= t_I + i\sum_K V_{I,K}(\sigma_K - i\alpha_K)\end{aligned} \tag{2.48}$$

6) Update: $\mathbf{U} \leftarrow \mathbf{U}_\sigma \mathbf{U}$, where $\mathbf{U}_\sigma = e^{i\sigma^T V \alpha \Delta\beta / N_e} e^{-\mathbf{h}_\sigma \Delta\beta}$ is the evolution matrix as discussed in step 5 of the AFMC algorithm in the previous section.

7) $l \leftarrow l + 1$. If $l < L$, go to step 4.

8) Update average $S \leftarrow \frac{S \times N_{iter} + \det \mathbf{F}^\dagger \mathbf{U} \mathbf{F}}{N_{iter} + 1}$ and iteration number $N_{iter} \leftarrow N_{iter} + 1$.

The huge effect of the shift on the statistics of a 2-site Hubbard model is seen in FIG. 1. We discuss more in detail the shifted contour and the Hubbard model in the next section. For a molecular system, where there is no real discrete auxiliary field analog, the shifted contour makes a huge difference; we discuss some examples in section IV.

The formalism of a new method to handle the sign problem is presented in Appendix B. This method is relies on the concept of coarse graining. Applications using this method will be discussed in a future publication.

3 Hubbard Model Energies

In the Hubbard model, the electron structure problem is studied in a simplified context: electrons "live" on a discrete (say, a 2 dimensional) lattice. There is a coupling t between nearest neighbor sites, so that electrons can hop from one site to its neighbor. The sites on the lattice are all equivalent so that the model has discrete translational symmetry and periodic boundary conditions are imposed. The electron-electron interaction is also very simplified. It is short ranged, so electrons on different sites *do not interact*. Electrons on the same site (and necessarily of opposite spins) repel each other, increasing the energy by U units. The Hubbard Hamiltonian is then:

$$\hat{H} = -t\sum_{\langle i,j\rangle}\sum_{\sigma=\downarrow\uparrow}\hat{c}^{\dagger}_{\sigma j}\hat{c}_{\sigma i} + U\sum_{j}\hat{n}_{\uparrow j}\hat{n}_{\downarrow j}\ . \tag{3.1}$$

In this expression, the first summation, in the so-called "one body term", is performed over all nearest-neighbor pairs of sites on the lattice. In the second Hamiltonian term, the electron number operators are $\hat{n}_{js} = \hat{c}^{\dagger}_{js}\hat{c}_{js}$. This term contains explicit particle-particle interactions and is thus called "a two-body term". We impose periodic boundary conditions on the system, making all sites equivalent with translational invariance. This means that sites on opposite boundaries of the lattice are considered "nearest neighbors". For a given lattice (say, a $N\times N$ 2D square lattice), all groundstate properties of the system depend on only three quantities: the ratio U/t (here, we agree to take $t=1$ in all subsequent applications) and the densities of electrons $n_s = N_s/M$ for $s=\uparrow,\downarrow$, where *M* is the number of sites on the lattice. In this review, we treat only closed shell systems, for which all electrons are paired, so that we need consider only two parameters: the parameter U and the electron density, n/M. In Hubbard model terminology, sometimes, people use the term "filling" which is the ratio of the number of electrons to the maximal number of electrons that can be accommodated by the lattice ($2N^2$). Thus, the case of density 1 is termed, "half filling". We should mention, en passé, that the 1D Hubbard problem (i.e. $N\times M$ lattices where *M* is small, typically *M* = 1, 2 or 3) can be treated using the density matrix renormalization group [26]. Lattice models of dimensionality greater than 2 are usually considered less difficult, because mean-field theories, such as the Hartree-Fock theory, perform well there.

Because for fermions $\hat{n}^2_{js} = \hat{n}_{js}$, the interaction term in the Hamiltonian can be written as $\hat{n}_{i\uparrow}\hat{n}_{i\downarrow} = \frac{1}{2}\left(\rho^2_{ii} - \rho_{ii}\right)$. This shows, by comparing with Eqs. (2.16) and (2.2) that the Hubbard model is an electronic structure type Hamiltonian with a particular choice of the parameter matrices T_{ij} and V_{ijkl}:

$$T_{ij} = -t\Delta_{ij} \qquad V_{ijkl} = U\delta_{ij}\delta_{kl}\delta_{ki}\ . \tag{3.2}$$

Where $\Delta_{ij} = 1$ if lattice site *i* is a neighbor of lattice site *j* and $\Delta_{ij} = 0$ for all other cases.

Even with the great simplifications introduced by the Hubbard model, the computational problem is of a formidable complexity, scaling exponentially as $4^{(\#\text{ of sites})}$. Over the years, several approaches have been developed for computing the electronic properties of finite sized model, aiming to obtain the picture of infinite lattices. Exact diagonalization methods serve as benchmarks for the small systems[27]. For larger systems, approximations are needed. The basic AFMC method for the Hubbard model was developed by Hirsch[15]. Hirsch's approach computes the partition function of the Hubbard electrons by employing the Hubbard-Stratonovich transformation. Because the special properties of the Hubbard model Hirsch's auxiliary fields take just two real values: ±1.

The general AFMC method we use does not make these special assumptions. Yet, our method does benefit from the special properties of the Hubbard model. In the Hubbard model, it is the exact density and not the entire *density matrix, which* is need for stabilization. This is so because within the Hubbard model the V-matrix is diagonal:

$$V_{I,K} = U\delta_{I,K}\delta_{ik}, \tag{3.3}$$

where $I = (ij)$ and $K = (kl)$, so the auxiliary fields are simpler than in the general case:

$$\sigma_I = \delta_{ij}\sigma_i. \tag{3.4}$$

The contour shift, α in the Hubbard model is therefore just the density, which is known exactly:

$$\alpha_i = n_i = \frac{N_e}{N}. \tag{3.5}$$

Thus, in the Hubbard model, the contour shift is just a shift by a constant! The huge effect this trivial shift makes is seen well in FIG. 1. By using this shift, we can perform accurate Monte Carlo on large size lattices with a large number of electrons. For example, we show in FIG. 2 the successful application to the 4×4 Hubbard model with $U = 8$ (we take $t = 1$ in all discussions).

By performing the computation on several computers, one is able to estimate the statistical error bars. The computation was carried out for up to $\beta = 0.7$. By a generalized least squares procedure, a best fit exponential was fit to the data points with $\beta > 0.25$, yielding a $\beta = \infty$ estimate of the energy, $E_\infty / N = -1.0931 \pm 0.0005$ where the error bar reflects the statistical error (there is also a systematic error associated with the extrapolation procedure). The exact, diagonalization-type result is[18] $E_\infty = -1.0944$. This shows that AFMC can give reliable and accurate results.

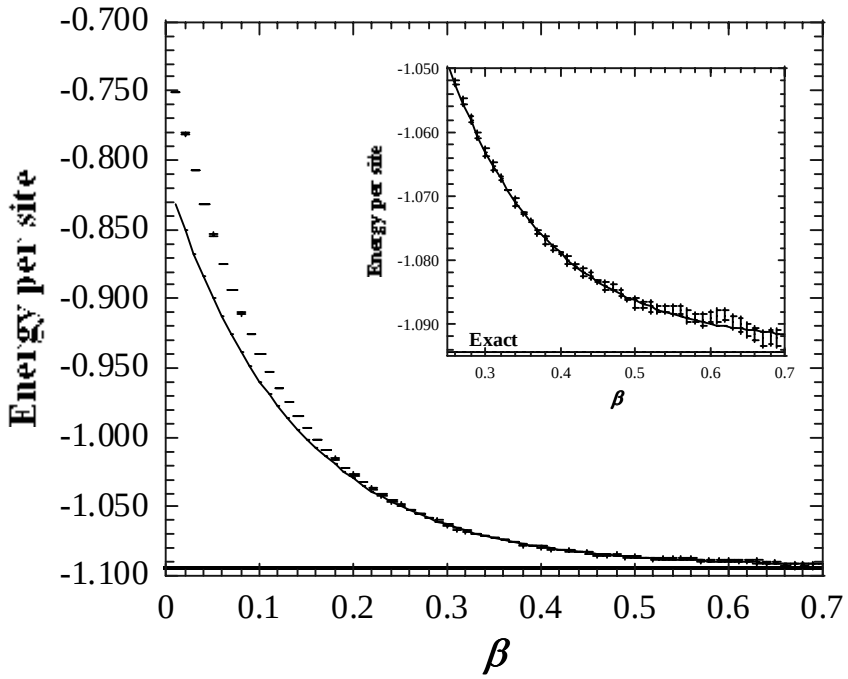

FIG. 2: The SC-AFMC energy of a 4×4 lattice with $t = 1$, $U = 8$ and 10 electrons ($N_\uparrow = N_\downarrow = 5$). The insert shows the details of the Monte-Carlo fluctuations. 40 Pentium III computers , each performing 1×10^6 iterations, were used for the computation.

An example far beyond the capabilities of exact diagonalization is the 16×16 lattice with 202 (101 spin-up and 101 spin-down) electrons. The results are shown in FIG. 3. A best fit exponential is fitted to the computation from which groundstate energy can be derived: $E/N = -1.135 \pm 0.01$. The error bar is only a statistical error. There is also an extrapolation error, which is more difficult to estimate. The constrained path Monte Carlo (CPMC) method[18] applied to the same problem yields $E/N = -1.1193 \pm 0.0003$. The CPMC has no sign error, so the statistical errors are very small. There is however an unknown systematic error, usually small, typically up to 0.01 energy units per site.

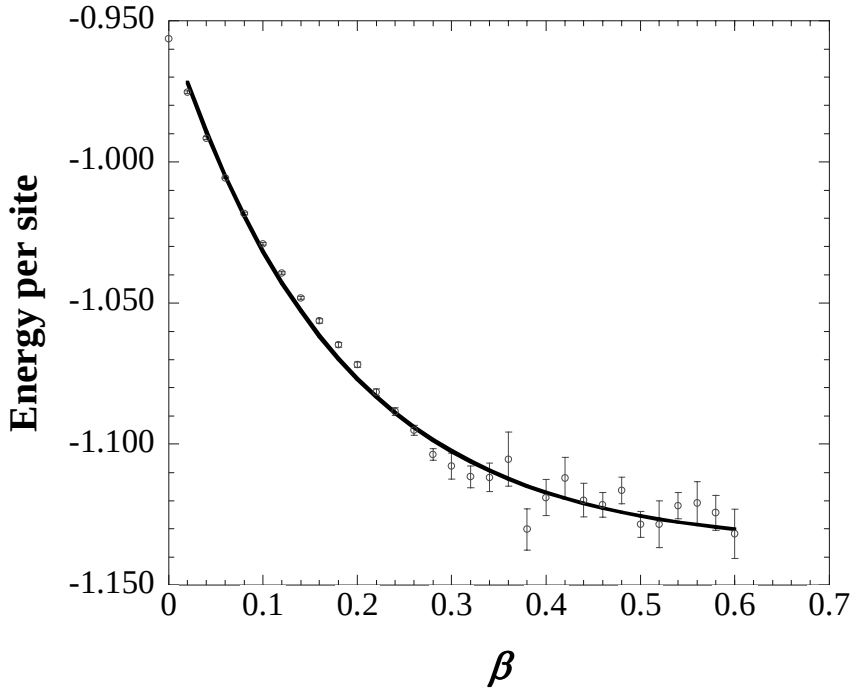

FIG. 3: The SC-AFMC energy of a 16×16 Hubbard lattice with 202 electrons. 150,000 iterations. The solid line is a best-fit exponential.

4 Quantum Chemistry Applications

This section is devoted to presenting some applications of SC-AFMC. We first discuss applications within a plane-waves basis for representing the one-electron wave functions and then applications within a Gaussian basis set.

For the plane waves applications, the molecule is placed in a cubic cell of length L, and a 3-dimensional grid of spacing Δx. The technique of Martyna et al.[28] is used for efficiently mitigating finite cell size effects. Computations employ either LSDA or B-LYP[29,30] based Troulier-Martins type[31] pseudopotentials, generated by the FHIPP98 computer program of Fuchs and Scheffler[32]. The pseudopotentials are non-local with $l_{\max} = 2$ and the Kleinman-Bylander form[33] is used for their efficient application in the code.

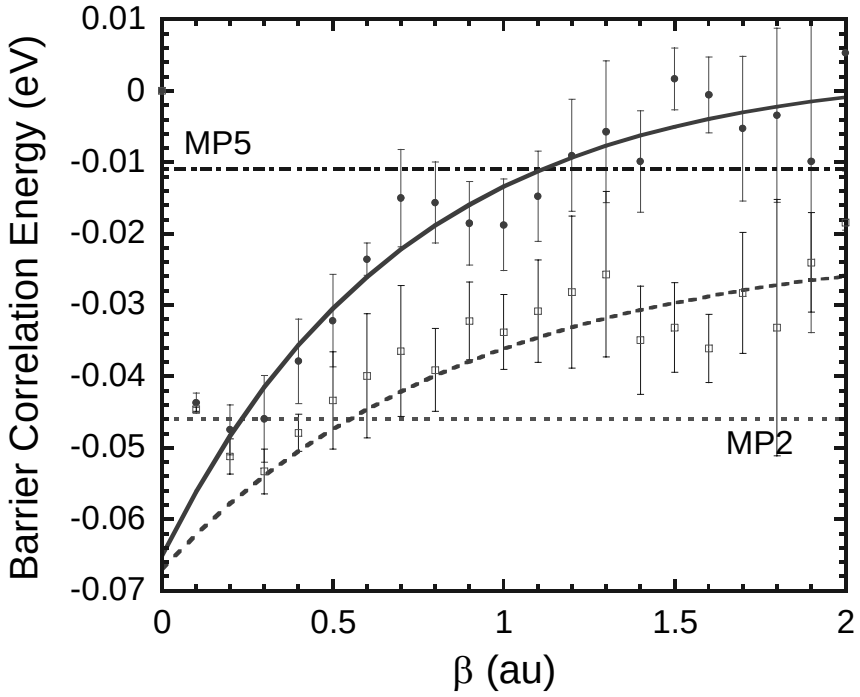

FIG. 4: The correlation energy contribution to the inversion barrier of water. It is seen that to within a statistical error of 0.01 eV the correlation energy is 0.00 eV. Taken from ref. [34].

The first application we discuss is the computation of the inversion barrier of water (FIG. 4). Taking into account correlation energy changes very little in the Hartree-Fock barrier height of 1.37eV. For small β values, it seems as if correlation energy lowers the barrier height. However at larger values of β this effect is counteracted. A similar picture emerges from perturbation theory computations of Tarczay et al[35], also shown in the figure.

The computation is made possible by correlated sampling, accomplished by using the same auxiliary fields for both the groundstate and the linear nuclear configurations. The auxiliary fields are sampled from a universal distribution, and therefore are not sensitive to nuclear position or even spin state.

A further application of correlated sampling is the calculation of spectroscopic constants of the N_2 molecule. Here, five nuclear configurations were correlated, and the results compared to the potential energy surface (PES) of Ref. [36]. The convergence as β is increased is clearly seen.

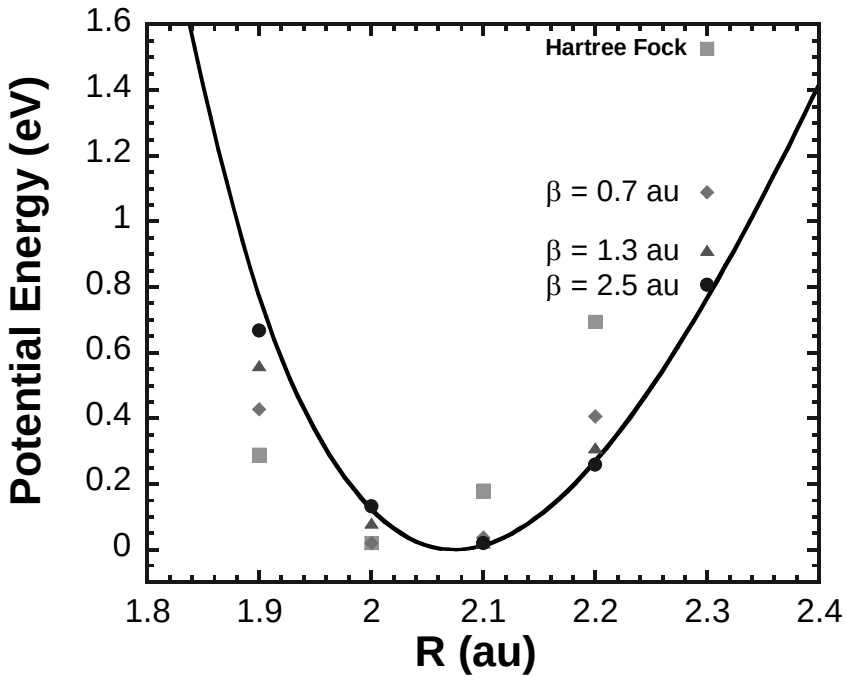

FIG. 5: Convergence of PES with increasing β. The solid line is a cubic spline through ab initio energy differences of Ref. [36] (the minimum of energy is taken as zero). Statistical errors in correlated energy differences of the largest β are ±0.03 eV (note that the statistical errors of absolute energy are ±0.18eV). Taken from ref. [37].

Correlated sampling can be used also for computing *energy differences* between ground and excited electronic states. For this we describe a variational multi-reference AFMC [23,38,39]. Consider a set of M determinantal wave functions $\Phi_m\left(\xi_1,\ldots,\xi_{N_e}\right)$, $m=1,\ldots,M$, the choice of which is application dependent, as discussed in the next section. Here ξ_n is the coordinates and spin of the nth electron.

Projecting with the Boltzmann operator, damping the high-energy components, a new set of M functions is obtained:

$$\Phi_m\left(\beta\right)=e^{-\beta\hat{H}}\Phi_m \ . \tag{3.6}$$

A linear combination of the resulting wave functions can efficiently approximate the true groundstate wave function:

$$\Psi_{gs}\approx\Psi=\sum_{m=1}^{M}C_m\Phi_m\left(\beta\right). \tag{3.7}$$

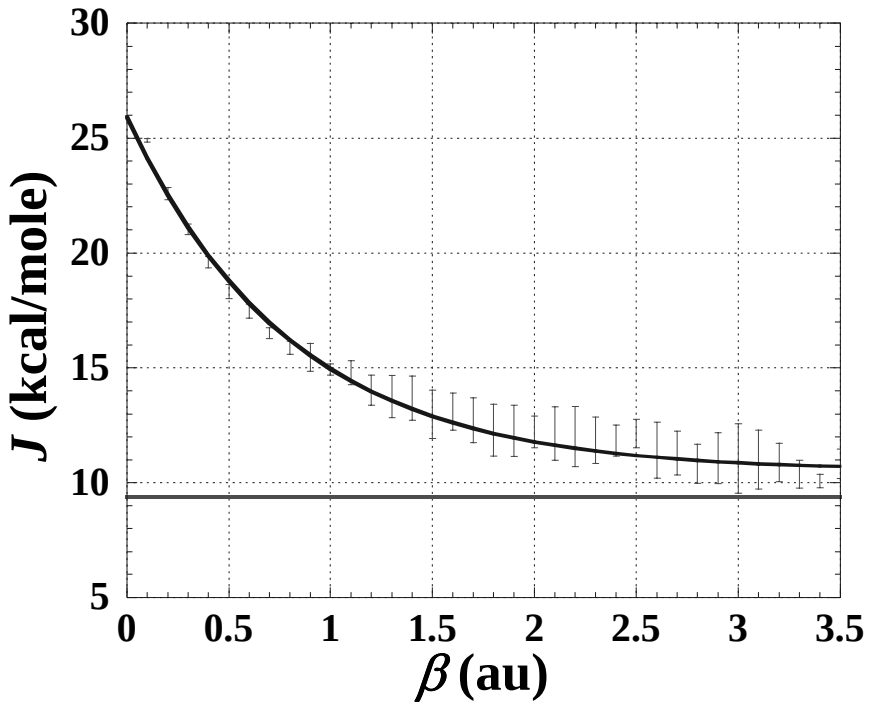

FIG. 6: Correlated sampling SC-AFMC computation of the Triplet-Singlet splitting for the methylene molecule. The full line is a best-fit exponential to the results for $\beta > 0.1$ au. The horizontal line is the relevant experimental result. The extrapolated $\beta \to \infty$ splitting is $J = 10.5 \pm 0.8$ kcal/mole. Cell length is $L = 12$ Bohr; grid spacing $\Delta x = 0.4$ Bohr and time step is $\Delta\beta = 0.1$ au. Total of 8,000 Monte Carlo iterations. Taken from ref. [39].

The coefficients C_m are determined by the variational principle, according to which:

$$E_{gs} \le \langle \Psi | \hat{H} | \Psi \rangle , \tag{3.8}$$

when $\langle \Psi | \Psi \rangle = 1$. Thus, the best coefficients are determined by minimizing the energy expectation value, subject to wave function normality. This amounts to minimizing the following functional:

$$J(\mathbf{C}) = \mathbf{C}^{\dagger}\mathbf{H}\mathbf{C} - \varepsilon \left\{ \mathbf{C}^{\dagger}\mathbf{S}\mathbf{C} - 1 \right\} , \tag{3.9}$$

where, a matrix-vector notation is employed, for example:

$$\mathbf{C}^{\dagger}\mathbf{S}\mathbf{C} = \sum_{m,m'=1}^{M} C_{m'}^{*} S_{m'm} C_m , \tag{3.10}$$

the Lagrange parameter ε multiplies the normalization constraint and the matrices appearing in Eq. (3.10) are computed using SCAFMC with the shift determined by

the density of the *right* determinant. The constrained minimization leads to the following generalized eigenvalue equation:

$$\mathbf{HC} = \mathbf{SCE}. \tag{3.11}$$

Where $\mathbf{E}$ is the diagonal matrix of Lagrange multipliers. The smallest Lagrange multiplier is the variational estimate for the ground state energy. Indeed, the following inequality exist in the limit of large β:

$$E_{gs} \le E(\beta) < E_{gs} + E_{M+1} e^{-\beta(E_{M+1}-E_{gs})}. \tag{3.12}$$

Estimates for low-lying excitation energies are given by the other diagonal elements of the matrix **E**.

We apply this method to CH_2 singlet-triplet level splitting done at the experimentally known C_{2v} geometries[40]: for the triplet state $R_{CH} = 1.075\,\text{Å}$ / $\theta_{HCH} = 133.9^\circ$ and for the singlet, $R_{CH} = 1.107\,\text{Å}$ and $\theta_{HCH} = 102.4^\circ$. A Hartree-Fock computation determines, for each spin state, the determinantal wave functions to be used as references for the QMC process. The references for the singlet and triplet states were the closed shell (S = 0) restricted Hartree-Fock (RHF) and the $S_z = 1$ unrestricted Hartree-Fock (UHF) determinants respectively. Correlated sampling is very efficient here, despite the fact that the two determinants are for different geometries *and* spin-orbitals. The resulting singlet-triplet energy difference of the CH_2 radical is shown in FIG. 6.

Table 1: Absolute energies of ethane at C-C bond length and large C-C separation. The energies were computed using SCAFMC and quadratic configuration interaction using singles and doubles[41] (a non-variational method). Based on Rom et al. [42]. The number of orbitals refers to the active space used.

N_{orb}	Method	$E_{R=1.54Å}$ (Ht)	$E_{R=3.54Å}$ (Ht)	ΔE (kcal/ mole)
15	SCAFMC	-79.245	-79.099	91.6
15	QCISD(T)	-79.245	-79.103	89.1
20	SCAFMC	-79.308	-79.156	94.7
20	QCISD(T)	-79.307	-79.159	92.9
28	SCAFMC	-79.414	-79.271	89.5
28	QCISD(T)	-79.417	-79.274	89.7

We now present some applications of AFMC using a Gaussian basis set framework. Here SCAFMC can be compared directly to other high level configuration interaction (CI) and coupled cluster (CC) methods. The C-C bond stretch energies of ethane are shown in Table 1.

Finally, we show an application addressing the excited state energies of the Neon atom, based on Rom et al.[23], shown in Table 2. The high quality of the Monte-Carlo excited state energies is seen by comparing to a matching full-CI calculation. The variational SC-AFMC was used for this computation.

Table 2: Ground and excited electronic state energies (Ht) of the Neon atom. Full-CI and variational SCAFMC at β = 1 au are compared. 9000 iterations of $\Delta\beta$ = 0.1 au and β_{max} = 1 au were performed on 9 determinantal references. Basis set was 4-31G. The numbers in parenthesis estimate the last digit statistical errors. From Rom et al. [22].

m	$E_m(\beta = 0)$	$E_m(\beta = 1au)$	E_m(full-CI)
0	0.000	-0.116(4)	-0.116
1	1.639	1.563(4)	1.562
2	1.782	1.713(4)	1.712
3	1.782	1.713(4)	1.712
4	1.868	1.802(4)	1.800
5	1.869	1.802(4)	1.800
6	2.606	2.42(2)	2.432
7	3.11	3.02(1)	3.02
8	3.46	3.26(2)	3.27

5 Summary

In this review, we have described the principles of a new electronic structure method - the shifted-contour auxiliary field Monte Carlo. We have described in detail the basic theory and algorithms, including the motivation and success of the contour shift. Mathematical techniques, which we felt were not covered in standard quantum chemistry texts were outlined in some detail.

We presented selected applications that show the method is capable of describing accurately electronic properties of molecules. The method was extended beyond chemical molecular structure to the realm of lattice models and strongly correlated electrons. Applications to large scale Hubbard models were given in this context.

Acknowledgements

This work was supported by the Israel Science Foundation founded by the Israel Academy of Sciences and Humanities.

Appendix A: Determinantal matrix elements

We now develop the necessary mathematical expressions for computing matrix elements of many-body operators between determinantal wave functions of the form similar to Eq. (2.7). We first assume that each determinant is composed of spin-orbitals $f_i(\mathbf{x})$ where $\mathbf{x}$ refers to both spin and space coordinates.

First, we discuss the overlap of two determinantal wavefunctions. As we shall see, the *overlap matrix*, $\left(g^\dagger f\right)_{\alpha\beta} \equiv \left\langle g_\alpha \middle| f_\beta \right\rangle$ plays an important role here. Consider

first the case where the orbitals of the left determinant are bi-orthogonal to those of the right determinant:

$$\left\langle g_\alpha \middle| f_\beta \right\rangle = \delta_{\alpha\beta}\sigma_\beta \,, \tag{A.1}$$

The *determinantal overlap* $\left\langle \Phi_g \middle| \Phi_f \right\rangle$ *is of a sum over all* permutations $\{p_\alpha\}$ and $\{q_\alpha\}$ of the terms $(N!)^{-1}(-)^{\{p_\alpha\}+\{q_\alpha\}}\prod_{\alpha=1}^{N_e}\left\langle g_{q_\alpha} \middle| f_{p_\alpha} \right\rangle$. If the functions are bi-orthogonal, the vast majority of such terms is zero and the determinantal overlap is simplified to the following expression*:*

$$\left\langle \Phi_g \middle| \Phi_f \right\rangle = \prod_{\alpha=1}^{N_e}\sigma_\alpha \,. \tag{A.2}$$

In general, the orbitals are not bi-orthonormal. However, there is a freedom to exploit. Consider a linear transformation that mixes the orbitals of a determinantal wave function:

$$\left| \tilde{f}_\alpha \right\rangle = \sum \left| f_\beta \right\rangle V_{\beta\alpha} \,. \tag{A.3}$$

Where, the matrix $\mathbf{V}$ is non-singular ($\det \mathbf{V} \neq 0$). Because of the general rule for square matrices, according to which: $\det \mathbf{A} \times \mathbf{V} = \det \mathbf{A} \det \mathbf{V}$, the following relation between the determinantal wave functions exists:

$$\left| \Phi_{\tilde{f}} \right\rangle = \left| \Phi_f \right\rangle \det V \,.$$

Thus, the wavefunction is only changed by a numeric factor. This freedom can now be used to bring the orbitals into bi-orthogonality, by rotating the left and right orbitals. The device of singular value decomposition (SVD)[25] proves especially useful here. The overlap matrix $\left(g^\dagger f\right)$ can be decomposed as follows:

$$\left(g^\dagger f\right) = U\Sigma V^\dagger \,, \tag{A.4}$$

where, U and V are unitary matrices, $U^\dagger U = UU^\dagger = VV^\dagger = V^\dagger V = I$ and Σ is a diagonal matrix with non-negative real diagonal matrix elements, called the *singular values*, appearing in ascending order: $\sigma_1 \geq \sigma_2 \geq \cdots \geq \sigma_{N_e}$. The decomposition is unique (except for the obvious cases that occur when there are identical singular values). The number of zero singular values is indicative of the way to treat determinantal matrix elements.

The matrices U and V are now used for defining two new sets of rotated orbitals of the left and right determinants:

$$\left| \tilde{g}_\alpha \right\rangle = \sum_{\alpha=1}^{N_e} U_{\alpha\beta} \left| g_\beta \right\rangle, \quad \left| \tilde{f}_\alpha \right\rangle = \sum_{\alpha=1}^{N_e} V_{\alpha\beta} \left| f_\beta \right\rangle. \tag{A.5}$$

The new orbitals are bi-orthogonal, as required by Eq. (A.1):

$$\left\langle \tilde{g}_\alpha \left| \tilde{f}_\beta \right\rangle = \sum_{\alpha',\beta'=1}^{N_e} \left(U^\dagger\right)_{\alpha\alpha'} \left\langle \tilde{g}_{\alpha'} \left| \tilde{f}_{\beta'} \right\rangle V_{\beta'\beta} = \delta_{\alpha\beta}\sigma_\beta \right. . \right. \tag{A.6}$$

The determinantal wave functions of the rotated orbitals equal to the original determinantal wave functions, multiplied at most by a phase factor:

$$\left|\Phi_{\tilde{g}}\right\rangle = \left|\Phi_g\right\rangle e^{i\theta_U} \quad , \quad \left|\Phi_{\tilde{f}}\right\rangle = \left|\Phi_f\right\rangle e^{i\theta_V} \, , \tag{A.7}$$

where θ_U and θ_V are real and $e^{i\theta_U} = \det U$ and $e^{i\theta_V} = \det V$ .We will denote the following product of the singular values:

$$\Delta_\alpha = \prod_{\beta=1}^{\alpha} \sigma_\beta \, . \tag{A.8}$$

Thus, the overlap of the original determinantal wave function is clearly:

$$\left\langle \Phi_g \left| \Phi_f \right\rangle = e^{i(\theta_U - \theta_V)} \Delta_{N_e} \right. . \tag{A.9}$$

Using the rotated orbitals, the matrix elements of a one-body operator:

$$\hat{T} = \sum_{n=1}^{N_e} \hat{t}\left(\mathbf{r}_i\right), \tag{A.10}$$

are readily computed. If all the singular values are non zeros, then:

$$\left\langle \Phi_g \left| \hat{T} \right| \Phi_f \right\rangle = e^{i(\theta_U - \theta_V)} \left\langle \Phi_{\tilde{g}} \left| \hat{T} \right| \Phi_{\tilde{f}} \right\rangle = e^{i(\theta_U - \theta_V)} \Delta_{N_e} \sum_{\alpha=1}^{N_e} \frac{t_\alpha}{\sigma_\alpha} \, . \tag{A.11}$$

With:

$$t_\alpha = \left\langle \tilde{g}_\alpha \left| \hat{t} \right| \tilde{f}_\alpha \right\rangle . \tag{A.12}$$

If there is one zero singular value then:

$$\left\langle \Phi_g \left| \hat{T} \right| \Phi_f \right\rangle = e^{i(\theta_U - \theta_V)} \Delta_{N_e - 1} t_{N_e} \, . \tag{A.13}$$

If there are more than one singular value, the matrix element is strictly zero.
Next, the matrix elements of a two-body operator are considered.

$$\hat{V} = \tfrac{1}{2} \sum_{\substack{n,m=1 \\ n \neq m}}^{N_e} \hat{v}\left(\mathbf{r}_n, \mathbf{r}_m\right) . \tag{A.14}$$

If all the singular values are non zeros, then:

$$\left\langle \Phi_g \left| \hat{V} \right| \Phi_f \right\rangle = e^{i(\theta_U - \theta_V)} \Delta_{N_e}^2 \tfrac{1}{2} \sum_{\alpha,\beta=1}^{N_e} \frac{v_{\alpha\alpha\beta\beta} - v_{\alpha\beta\beta\alpha}}{\sigma_\alpha \sigma_\beta} \, , \tag{A.15}$$

where:

$$\begin{aligned} v_{\alpha\alpha\beta\beta} &= \int \tilde{g}_\alpha^*\left(\mathbf{x}_1\right) \tilde{f}_\alpha\left(\mathbf{x}_1\right) \hat{v}\left(\mathbf{r}_1, \mathbf{r}_2\right) \tilde{g}_\beta^*\left(\mathbf{x}_2\right) \tilde{f}_\beta\left(\mathbf{x}_2\right) dx_1 dx_2 \\ v_{\alpha\beta\beta\alpha} &= \int \tilde{g}_\alpha^*\left(\mathbf{x}_1\right) \tilde{f}_\beta\left(\mathbf{x}_1\right) \hat{v}\left(\mathbf{r}_1, \mathbf{r}_2\right) \tilde{g}_\beta^*\left(\mathbf{x}_2\right) \tilde{f}_\alpha\left(\mathbf{x}_2\right) dx_1 dx_2 \end{aligned} \, . \tag{A.16}$$

If there is a single zero singular value, then

$$\left\langle \Phi_g \left| \hat{V} \right| \Phi_f \right\rangle = e^{i(\theta_U - \theta_V)} \Delta_{N_e - 1} \tfrac{1}{2} \sum_{\alpha=1}^{N_e} \frac{v_{N_e N_e \alpha\alpha} - v_{N_e \alpha\alpha N_e}}{\sigma_\alpha}, \tag{A.17}$$

and of there are two zero singular values:

$$\left\langle \Phi_g \left| \hat{V} \right| \Phi_f \right\rangle = \Delta_{N_e - 2} \tfrac{1}{2} \left(v_{N_e (N_e-1)(N_e-1) N_e} - v_{N_e (N_e-1) N_e (N_e-1)} \right). \tag{A.18}$$

The matrix element of a two body operator is zero if there are more than two zero singular values.

The expressions given up to now were general. We now specialize to the case assuming that the orbitals f_α can be expanded in terms of N orthonormal basis orbitals ϕ_j:

$$f_\alpha(\mathbf{x}) = f_\alpha(\mathbf{r}, \sigma) = \sum_{j=1}^{N} \sum_{s=\uparrow\downarrow} \phi_{js}(\mathbf{r}) \delta_{s,\sigma} F_{js,\alpha} \,. \tag{A.19}$$

The rectangular coefficient matrix $(\mathbf{F})_{js\alpha}$ is associated with the determinantal wavefunction of Eq. (2.7). Consider the overlap matrix:

$$\left\langle g_\alpha \middle| f_\beta \right\rangle = \left(\mathbf{G}^\dagger \mathbf{F} \right)_{\alpha\beta} \tag{A.20}$$

Once again we use the SVD of Eq. (A.4), yielding the unitary matrices U and V and the singular values $\sigma_1 \geq \sigma_2 \geq \cdots \geq \sigma_{N_e}$. Using the unitary matrices, we define the rotated coefficient matrices:

$$\tilde{\mathbf{G}} = \mathbf{G}U \,, \;\; \tilde{\mathbf{F}} = \mathbf{F}V \,. \tag{A.21}$$

Thus,

$$\tilde{\mathbf{G}}^\dagger \tilde{\mathbf{F}} = U^\dagger \mathbf{G}^\dagger \mathbf{F} V = \Sigma \,. \tag{A.22}$$

The equations (A.11), (A.13), (A.15), (A.17) and (A.18) can be used with the definitions:

$$t_\alpha = \left(\tilde{\mathbf{G}}^\dagger \mathbf{T} \tilde{\mathbf{F}} \right)_{\alpha\alpha}, \tag{A.23}$$

where, $(\mathbf{T})_{ij} = T_{ij}$ and for the 2-body operator:

$$\hat{V} = \tfrac{1}{2} \sum_{\substack{n,m=1 \\ n \neq m}}^{N_e} \hat{v}(\mathbf{r}_n, \mathbf{r}_m) \Leftrightarrow \tfrac{1}{2} \sum_{ijss'} V_{ijkl} \hat{c}_{is}^\dagger \hat{c}_{ks'}^\dagger c_{ls} c_{js} \,. \tag{A.24}$$

we have:

$$\begin{aligned} v_{\alpha\alpha\beta\beta} &= \sum_{ijkl,s,s'} \left(\tilde{\mathbf{G}}^\dagger \right)_{\alpha,is} \tilde{\mathbf{F}}_{js,\alpha} \left(\tilde{\mathbf{G}}^\dagger \right)_{\beta,ks'} \tilde{\mathbf{F}}_{ls',\beta} V_{ijkl} \\ v_{\alpha\beta\beta\alpha} &= \sum_{ijkl,s,s'} \left(\tilde{\mathbf{G}}^\dagger \right)_{\alpha,is} \tilde{\mathbf{F}}_{js,\beta} \left(\tilde{\mathbf{G}}^\dagger \right)_{\beta,ks'} \tilde{\mathbf{F}}_{ls',\alpha} V_{ijkl} \end{aligned} \,. \tag{A.25}$$

The quantities defined in Eqs. (A.23) and (A.25) should not be used in an actual computer implementation because of the high cost of affecting the transformation. Instead, the following economical expressions are given:

$$\left\langle \Phi_g \left| \hat{T} \right| \Phi_f \right\rangle = e^{i(\theta_U - \theta_V)} tr\mathbf{PT} = e^{i(\theta_U - \theta_V)} \sum_{ij,s} \mathbf{P}_{is,js} T_{ji} \,, \tag{A.26}$$

where, the density matrix $\mathbf{P}$ is defined as:

$$\mathbf{P} = \tilde{\mathbf{F}} \tilde{\Sigma} \tilde{\mathbf{G}}^{\dagger} \,. \tag{A.27}$$

Here, $\tilde{\Sigma}$ is the diagonal matrix with:

$$\tilde{W}_{\alpha\beta} = \delta_{\alpha\beta} \prod_{\gamma \neq \alpha} \sigma_\gamma \,. \tag{A.28}$$

Next, we treat 2-body operator. With all singular values being positive:

$$\left\langle \Phi_g \left| \hat{V} \right| \Phi_f \right\rangle = e^{i(\theta_U - \theta_V)} \tfrac{1}{2} \sum_{ijkl, s_1 s_2} \mathbf{P}_{is_1 js_1} \mathbf{P}_{ks_2 ls_2} v_{ijkl} - \mathbf{P}_{is_1 ls_2} \mathbf{P}_{ks_2 js_1} v_{ijkl} \,. \tag{A.29}$$

In Eq. (2.14) we discussed the matrix element of an evolution operator of a 1-body Hamiltonian $\left\langle \Phi_g \left| \hat{U}_\sigma \right| \Phi_f \right\rangle$. In principle, there are two venues to take here. The first, suitable to very large and sparse representation of the orbitals is to use a Chebyshev evolution method by Kosloff[43]. For computations within the orthonormal basis framework, the matrix representation $\left(\mathbf{U}_\sigma\right)_{ij} = \left\langle \phi_i \left| \hat{U}_\sigma \right| \phi_j \right\rangle$ of the evolution operator may be computed by matrix exponentiation:

$$\left(\mathbf{U}_\sigma\right)_{ik} = \left(e^{-i\mathbf{h}_\sigma \Delta\beta}\right)_{ik} = \sum_{j=1}^{N} \left(\mathbf{S}^{-1}\right)_{ij} e^{-iE_j \Delta\beta} \left(\mathbf{S}\right)_{jk} \,. \tag{A.30}$$

Where, the columns of the matrix $\mathbf{S}$ are the right eigenvectors of $\mathbf{h}_\sigma$. Consecutive operation of several evolution operators is done by matrix multiplication, $\mathbf{U} = \mathbf{U}_{\sigma_L} \cdots \mathbf{U}_{\sigma_1}$. Each of the orbitals of Φ_f is thus rotated by $\mathbf{U}$, after which the methods of SVD discussed above can be used.

For wavefunctions of spin-0, it is beneficial to compute determinantal matrix elements of closed-shell (CS) determinantal wavefunctions. The $N_e/2$ orbitals are represented by a matrix with respect to $\phi_j(\mathbf{r})$:

$$f_\alpha(\mathbf{r}) = \sum_{j=1}^{N} \phi_j(\mathbf{r}) F_{j,\alpha} \,. \tag{A.31}$$

Each orbital is occupied by a spin-up *and* spin-down electron. Thus:

$$\Phi_f^{CS} \equiv \Phi^{\uparrow}_{f_1 \cdots f_{N_e/2}} \Phi^{\downarrow}_{f_1 \cdots f_{N_e/2}} \,. \tag{A.32}$$

One can still define matrices as in (A.19)-(A.22). The overlap is now the square of the determinant:

$$\left\langle \Phi_g^{CS} \left| \Phi_f^{CS} \right\rangle = \Delta_{N_e/2}{}^2 \,. \tag{A.33}$$

The CS density matrix is defined similarly to Eq. (A.27). Note, that the relation between the CS and the regular density matrices is:

$$\mathbf{P}_{ij}^{CS} = \mathbf{P}_{i\uparrow, j\uparrow} = \mathbf{P}_{i\downarrow, j\downarrow} \,. \tag{A.34}$$

The one-body matrix element is:

$$\left\langle \Phi_g^{CS} \left| \hat{T} \right| \Phi_g^{CS} \right\rangle = e^{2i(\theta_U - \theta_V)} 2tr\mathbf{PT} = e^{2i(\theta_U - \theta_V)} 2\sum_{ij,s} \mathbf{P}_{is,js} T_{ji} \ . \tag{A.35}$$

The two-body operator matrix element is:

$$\left\langle \Phi_g^{CS} \left| \hat{V} \right| \Phi_f^{CS} \right\rangle = e^{2i(\theta_U - \theta_V)} \tfrac{1}{2} \sum_{ijkl} \mathbf{P}_{ij} \mathbf{P}_{kl} \left(4v_{ijkl} - 2v_{ilkj} \right). \tag{A.36}$$

Appendix B: Coarse graining

In this appendix, we develop a new approach toward improving AFMC by a coarse graining procedure of the SCAFMC integrand, based on the Filinov transform[44]. The basic idea is to use the identities:

$$\sqrt{a\Delta\beta/2\pi} \int_{-\infty}^{\infty} \exp\left(-\tfrac{1}{2} a y^2 \Delta\beta \right) dy = 1, \tag{B.1}$$

and:

$$\int \Gamma[\sigma] d\sigma = \int \Gamma[\sigma + y\zeta] d\sigma \ . \tag{B.2}$$

In the integral of Eq. (2.35), with

$$\Gamma[\sigma] = W[\sigma] \left\langle \Phi_g \left| \hat{U}_{\sigma_L} \cdots \hat{U}_{\sigma_1} \right| \Phi_f \right\rangle . \tag{B.3}$$

Thus:

$$S(\beta) = \int \Gamma[\sigma] D\sigma = \int \Gamma[\sigma] C[\sigma] D\sigma \ . \tag{B.4}$$

where:

$$\begin{aligned} C[\sigma]\Gamma[\sigma] &= \Xi[\sigma] \\ &= \sqrt{a\Delta\beta/2\pi} \int_{-\infty}^{\infty} \exp\left(-\tfrac{1}{2} a y^2 \Delta\beta \right) \Gamma[\sigma + y\zeta] dy \end{aligned} \ . \tag{B.5}$$

The integrand $\Xi[\sigma]$ is an average of $\Gamma[\sigma]$ in a given space-time "direction" ζ. It is expected to be coarse-grained, or less oscillatory. In the Filinov approach the constant *a* is taken large and the logarithm of Ξ is expanded as a Taylor series to second order. In the Hubbard Stratonovich formalism, this does not appear to be a practical route, and we therefore resort to a different approach. We now show, that by a judicious choice of the direction ζ, the integration on *y* in Eq. (B.5) can be performed analytically. We then give a new integrand that depends on ζ. The final Monte Carlo method then averages on all possible choices of ζ.

Before we describe the method, we discuss some important technical issues. We will, for simplicity, work in a closed shell framework. We denote by $\tilde{g}_\alpha(\mathbf{r})$ and $\tilde{f}_\alpha(\mathbf{r},\beta)$ the bi-orthogonal orbitals to the orbitals obtained from $g_\alpha(\mathbf{r})$ and $f_\gamma(\mathbf{r},\beta) = \hat{U}_{\sigma_L} \cdots \hat{U}_{\sigma_1} f_\gamma(\mathbf{r})$. The procedure for computing these bi-orthogonal orbitals has been discussed in detail in appendix **A**. It is important to note, that these

relations are *time-independent*, so using $\langle \tilde{g}_\alpha(\tau)| = \langle \tilde{g}_\alpha | \hat{U}_L \cdots \hat{U}_l$ where $\tau = l\Delta\beta$, one has:

$$\langle \tilde{g}_\alpha(\tau) | \tilde{f}_\beta(\tau) \rangle = \langle \tilde{g}_\alpha | \hat{U}_{\sigma_L} \cdots \hat{U}_{\sigma_1} | \tilde{f}_\beta \rangle = \sigma_\alpha \delta_{\alpha\beta} . \quad \text{(B.6)}$$

An additional technical detail concerns the density matrix: $\hat{\rho}_{I,s} = \hat{\rho}_{ij,s} = c_{is}^\dagger c_{js}$. The square of this operator is:

$$\hat{\rho}_{I,s}^2 = \hat{\rho}_{I,s} \delta_I , \quad \text{(B.7)}$$

where $\delta_I = \delta_{ij}$. For any function of a single variable $\phi(x)$, we have then:

$$\phi(\hat{\rho}_{I,s}) = \phi(0) + \tilde{\phi} \times \hat{\rho}_{I,s} , \quad \text{(B.8)}$$

with $\delta_I^c \equiv 1 - \delta_I$ and:

$$\tilde{\phi}_I = \left[\phi(1) - \phi(0) \right] \delta_I + \phi'(0) \delta_I^c . \quad \text{(B.9)}$$

This can be proved by formally expanding $\phi(x)$ in an infinite Taylor's series and using Eq. (B.7). In a closed-shell formalism, let us define the expectation value of a density matrix component as:

$$\langle \Phi_g(\tau) | \hat{\rho}_{I,s} | \Phi_f(\tau) \rangle \equiv \tilde{\rho}_I(\tau) . \quad \text{(B.10)}$$

In terms of the basis set components (see Eq. (A.27) for comparison):

$$\tilde{\rho}_I(\tau) \equiv \left(\tilde{\mathbf{F}}(\tau) \tilde{\Sigma}(\tau) \tilde{\mathbf{G}}(\tau)^\dagger \right)_I . \quad \text{(B.11)}$$

The expectation value of $\phi(\hat{\rho}_{I,s}) = \exp(i\alpha\hat{\rho}_{I,s})$ is:

$$\langle \Phi_g(\tau) | \exp(i\alpha\hat{\rho}_{I,s}) | \Phi_f(\tau) \rangle = 1 + \tilde{\phi}_I \tilde{\rho}_I(\tau) , \quad \text{(B.12)}$$

where:

$$\tilde{\phi}_I = \left(\exp(i\alpha) - 1 \right) \delta_I + i\alpha \delta_I^c . \quad \text{(B.13)}$$

For $\hat{\rho}_I = \hat{\rho}_{I\uparrow} + \hat{\rho}_{I\downarrow}$ we have $\exp(i\alpha\hat{\rho}_I) = \exp(i\alpha\hat{\rho}_{I,\uparrow}) \exp(i\alpha\hat{\rho}_{I,\downarrow})$ and thus:

$$\langle \Phi_g(\tau) | \exp(i\alpha\hat{\rho}_I) | \Phi_f(\tau) \rangle = \left[1 + \tilde{\phi}_I \tilde{\rho}_I(\tau) \right]^2 . \quad \text{(B.14)}$$

We now return to the derivation of the analytical integral of Eq. (B.5). The critical issue here is the choice of direction ζ.

We select an index I_0 and define ζ to correspond to it by:

$$(V\zeta)_I = \sum_J V_{IJ} \zeta_J = \delta_{I,I_0} . \quad \text{(B.15)}$$

The following identities hold:

$$\zeta^T V \sigma_{l_0} = \sigma_{I_0 l_0} , \; \zeta^T V \hat{\rho} = \hat{\rho}_{I_0} , \; \zeta^T V \zeta = \zeta_{I_0} . \quad \text{(B.16)}$$

The direction ζ is also time dependent. We choose it to be zero for all time slices except for the $l = l_0$ slice. With these definitions, we proceed to evaluate:

$$\sqrt{a\Delta\beta/2\pi}\int_{-\infty}^{\infty}\Gamma\left[\sigma+y\zeta\right]\exp\left(-\tfrac{1}{2}ay^2\Delta\beta\right)dy=$$
$$\sqrt{a\Delta\beta/2\pi}\Gamma\left[\sigma\right]\int_{-\infty}^{\infty}dy\exp\left(-\tfrac{1}{2}ay^2\Delta\beta\right)\times$$
$$\frac{\exp\left(-\tfrac{1}{2}\left(\sigma_{l_0}-y\zeta\right)^T V\left(\sigma_{l_0}-y\zeta\right)\Delta\beta\right)}{\exp\left(-\tfrac{1}{2}\sigma_{l_0}{}^T V\sigma_{l_0}\Delta\beta\right)}\times$$
$$\left\langle\Phi_g\left(t_{l_0}\right)\middle|\exp\left(iy\hat{\rho}_{I_0}\Delta\beta\right)\middle|\Phi_f\left(t_{l_0}\right)\right\rangle.$$

We now use Eq. (B.12) with $\phi(x)=\exp(iyx\Delta\beta)$ and obtain:

$$\Xi_{I_0l_0}\left[\sigma\right]/\Gamma\left[\sigma\right]=\sqrt{a\Delta\beta/2\pi}$$
$$\int_{-\infty}^{\infty}\exp\left(-\tfrac{1}{2}b\left[y^2-2y\,\sigma_{I_0,l_0}/b\right]\Delta\beta\right)\times \qquad \text{(B.17)}$$
$$\left[1+\tilde{\phi}_{I_0}\tilde{\rho}_{I_0,l_0}\right]^2 dy$$

where we define $b=a+\zeta_{I_0}$. Assume first I_0 is diagonal index ($I_0=(i_0i_0)$). Then, from Eq. (B.13) $\tilde{\phi}_{I_0}=e^{iy\Delta\beta}-1$ and the coarse graining function is:

$$\Xi_{I_0l_0}\left[\sigma\right]/\Gamma\left[\sigma\right]=\mathbf{K}_0+2\tilde{\rho}_{I_0l_0}\left(\mathbf{K}_1-\mathbf{K}_0\right)+\tilde{\rho}_{I_0l_0}^2\left(\mathbf{K}_0+2\mathbf{K}_1+\mathbf{K}_2\right), \qquad \text{(B.18)}$$

with

$$\mathbf{K}_k=\sqrt{a/b}\exp\left(\left[\sigma_{I_0l_0}+ik\right]^2/2b\right). \qquad \text{(B.19)}$$

Next, assume I_0 is a non-diagonal index. Then, $\tilde{\phi}=\phi'(0)=iy\Delta\beta$. In this case, the coarse graining function turns out to be:

$$\Xi_{I_0l_0}\left[\sigma\right]/\Gamma\left[\sigma\right]=\left(1+i\mathbf{J}_1\tilde{\rho}_{I_0l_0}+\mathbf{J}_2\tilde{\rho}_{I_0l_0}\right)\sqrt{a/b}\exp\left(\sigma_{I_0l_0}^2\Delta\beta/2b\right), \qquad \text{(B.20)}$$

with:

$$\mathbf{J}_1=\sigma_{I_0l_0}\Delta\beta/b\,,\quad \mathbf{J}_2=-\Delta\beta/b\left[1+\sigma_{I_0l_0}^2\Delta\beta/b\right]. \qquad \text{(B.21)}$$

The final expression for the coarse graining function is:

$$C\left[\sigma\right]=\frac{1}{LM}\sum_{I_0l_0}\Xi_{I_0l_0}\left[\sigma\right]/\Gamma\left[\sigma\right], \qquad \text{(B.22)}$$

to be used in Eq. (B.4).

Index

References

1. Kalos M. H., *Phys. Rev.* **128** (1962) pp. 560.
2. Kalos M. H., Levesque D., and Verlet L., *Phys. Rev. A* **9** (1974) pp. 2178.
3. McMillan W. L., *Phys. Rev. A.* **138** (1965) pp. 442.
4. Hammond B. L., Jr. W. A. L., and Reynolds P. J., *Monte Carlo Methods in ab initio quantum chemistry* (World Scientific, Singapore, 1994).
5. Anderson J. B., *J. Chem. Phys.* **63** (1975) pp. 1499.
6. Filippi C. and Umrigar C. J., Multiconfiguration wave functions for quantum Monte Carlo calculations of first-row diatomic molecules, *J. Chem. Phys.* **105** (1996) pp. 213-226.
7. Ceperley D. M. and Mitas L., Quantum Monte Carlo Methods in Chemistry, *Adv. Chem. Phys.* **93** (1996) pp. 1.
8. Luchow A. and Anderson J. B., Monte Carlo methods in electronic structures for large systems, *Annu. Rev. Phys. Chem.* **51** (2000) pp. 501-526.
9. Foulkes W. M. C., Mitas L., Needs R. J., and Rajagopal G., Quantum Monte Carlo simulations of solids, *Rev. Mod. Phys.* **73** (2001) pp. 33.

10. Filippi C. and Umrigar C. J., Correlated sampling in quantum Monte Carlo: A route to forces, *Phys. Rev. B* **61** (2000) pp. R16291-R16294.
11. Schautz F. and Flad H. J., Quantum Monte Carlo study of the dipole moment of CO, *J. Chem. Phys.* **110** (1999) pp. 11700-11707.
12. Ceperley D. M. and Alder B. J., *Phys. Rev. Lett.* **45** (1980) pp. 566.
13. Ceperley D. M., *J. Comput. Phys.* **51** (1983) pp. 404.
14. Mahan G. D., *Many-Particle Physics*, 3 ed. (Kluwer Academic/Plenum Publishers, New-York, 2000).
15. Hirsch J. E., *Phys. Rev. B* **31** (1985) pp. 4403.
16. Loh E. Y., Jr. and Gubernatis J. E., in *Electronic Phase Transitions*, Vol. 32, edited by W. Hanke and Y. V. Kopaev (North-Holland, Amsterdam, 1992).
17. Zhang S. W., Carlson J., and Gubernatis J. E., Constrained Path Quantum Monte-Carlo Method for Fermion Ground- States, *Phys. Rev. Lett.* **74** (1995) pp. 3652-3655.
18. Zhang S. W., Carlson J., and Gubernatis J. E., Constrained path Monte Carlo method for fermion ground states, *Phys. Rev. B* **55** (1997) pp. 7464-7477.
19. Sugiyama G. and Koonin S. E., *Ann. Phys. N.Y.* **168** (1986) pp. 1.
20. Koonin S. E., Dean D. J., and Langanke K., Shell model Monte Carlo methods, *Phys. Rep.-Rev. Sec. Phys. Lett.* **278** (1997) pp. 2-77.
21. Silvestrelli P. L., Baroni S., and Car R., Auxiliary-Field Quantum Monte-Carlo Calculations for Systems with Long-Range Repulsive Interactions, *Phys. Rev. Lett.* **71** (1993) pp. 1148-1151.
22. Charutz D. M. and Neuhauser D., Electronic-Structure Via the Auxiliary-Field Monte-Carlo Algorithm, *J. Chem. Phys.* **102** (1995) pp. 4495-4504.
23. Rom N., Charutz D. M., and Neuhauser D., Shifted-contour auxiliary-field Monte Carlo: Circumventing the sign difficulty for electronic-structure calculations, *Chem. Phys. Lett.* **270** (1997) pp. 382-386.
24. Baer R., Head-Gordon M., and Neuhauser D., Shifted-contour auxiliary field Monte Carlo for ab initio electronic structure: Straddling the sign problem, *J. Chem. Phys.* **109** (1998) pp. 6219-6226.
25. Golub G. H. and van Loan C. F., *Matrix Computations*, 3 ed. (The John Hopkins University Press, Baltimore, 1996).
26. White S. R., Strongly correlated electron systems and the density matrix renormalization group, *Phys. Rep.-Rev. Sec. Phys. Lett.* **301** (1998) pp. 187-204.
27. Soos Z. G. and Ramasesha S., *Phys. Rev. B* **29** (1984) pp. 5410.
28. Martyna G. J. and Tuckerman M. E., A reciprocal space based methods for treating long range interactions in ab initio and force field based calculations in clusters, *J. Chem. Phys.* **110** (1999) pp. 2810-2821.
29. Becke A. D., Density-Functional Exchange-Energy Approximation with Correct Asymptotic-Behavior, *Phys. Rev. A* **38** (1988) pp. 3098-3100.

30. Lee C. T., Yang W. T., and Parr R. G., Development of the Colle-Salvetti Correlation-Energy Formula into a Functional of the Electron-Density, *Phys. Rev. B* **37** (1988) pp. 785-789.
31. Troullier N. and Martins J. L., Efficient Pseudopotentials for Plane-Wave Calculations, *Phys. Rev. B* **43** (1991) pp. 1993-2006.
32. Fuchs M. and Scheffler M., Ab initio pseudopotentials for electronic structure calculations of poly-atomic systems using density-functional theory, *Comput. Phys. Commun.* **119** (1999) pp. 67-98.
33. Kleinman L. and Bylander D. M., *Phys. Rev. Lett.* **48** (1982) pp. 1425.
34. Baer R., Ab-initio molecular deformation barriers using auxiliary-field quantum Monte Carlo with application to the inversion barrier of water, *Chem. Phys. Lett.* **324** (2000) pp. 101-107.
35. Tarczay G., Csaszar A. G., Klopper W., Szalay V., Allen W. D., and Schaefer H. F., The barrier to linearity of water, *J. Chem. Phys.* **110** (1999) pp. 11971-11981.
36. Gdanitz R. J., Accurately solving the electronic Schrodinger equation of atoms and molecules using explicitly correlated (r(12)-) MR-CI: the ground state potential energy curve of N-2, *Chem. Phys. Lett.* **283** (1998) pp. 253-261.
37. Baer R., Ab initio computation of forces and molecular spectroscopic constants using plane waves based auxiliary field Monte Carlo with application to N-2, *J. Chem. Phys.* **113** (2000) pp. 473-476.
38. Bernu B., Ceperley D. M., and Lester W. A., The Calculation of Excited-States with Quantum Monte-Carlo .2. Vibrational Excited-States, *J. Chem. Phys.* **93** (1990) pp. 552-561.
39. Baer R., Ab Initio computation of singlet-triplet molecular energy differences using Auxiliary Field Monte Carlo, *Chem. Phys. Lett.* **in press** (2001).
40. Petek H., Nesbitt D. J., Darwin D. C., Ogilby P. R., Moore C. B., and Ramsay D. A., Analysis of Ch2a 1a1 (1,0,0) and (0,0,1) Coriolis-Coupled States, a 1a1-X 3b1 Spin Orbit Coupling, and the Equilibrium Structure of Ch2a 1a1 State, *J. Chem. Phys.* **91** (1989) pp. 6566-6578.
41. Dupuis M., Rys J., and King H. F., *J. Chem. Phys.* **65** (1976) pp. 111.
42. Rom N., Fattal E., Gupta A. K., Carter E. A., and Neuhauser D., Shifted-contour auxiliary-field Monte Carlo for molecular electronic structure, *J. Chem. Phys.* **109** (1998) pp. 8241-8248.
43. Kosloff R., Time-Dependent Quantum-Mechanical Methods for Molecular- Dynamics, *J. Phys. Chem.* **92** (1988) pp. 2087-2100.
44. Filinov V. S., *Nuclear Physics B* **271** (1986) pp. 717.